

Significance of Fidelity Deviation in Continuous Variable Teleportation

Ayan Patra¹, Rivu Gupta¹, Saptarshi Roy^{1,2,3}, and Aditi Sen(De)¹

¹Harish-Chandra Research Institute, A CI of Homi Bhabha National Institute, Chhatnag Road, Jhansi, Prayagraj - 211019, India

²Quantum Information and Computation Initiative, Department of Computer Science,
The University of Hong Kong, Pokfulam Road, Hong Kong, and

³HKU-Oxford Joint Laboratory for Quantum Information and Computation.

Performance of quantum teleportation is typically measured by the average fidelity, an overlap between the input and output states. Along with the first moment, we introduce the second moment of fidelity in CV teleportation, i.e., the fidelity deviation as the figures of merit to assess the protocol's efficiency. We show that CV states, both Gaussian and non Gaussian, can be better characterized by considering both average fidelity and fidelity deviation, which is not possible with only average fidelity. Moreover, we shed light on the performance of the teleportation protocol in two different input scenarios - one is when input states are sampled from constrained uniform distribution while the other one is Gaussian suppression of the input states which again lead to a different classification of CV states according to their performance. The entire analysis is carried out in noiseless and noisy scenarios with noise being incorporated in the measurement and the shared channels. We also report that one type of noise can make the protocol robust against the other one which leads to a 'constructive effect' and identify the noise models which are responsible for decreasing average fidelity and increment in fidelity deviation.

I. INTRODUCTION

Quantum teleportation (QT), discovered in 1993 [1] is unmistakably one of the remarkable pieces of sorcery that quantum mechanics makes possible. After its proposal, it has tasted unprecedented levels of success both theoretically [2–7] and experimentally [8–17] in its mere two decade long existence. The latest feather in the cap of experimental QT is undoubtedly the satellite-based setups that give rise to a possibility of realizing quantum information transmission at intercontinental distances [16, 18, 19]. Interestingly, this tremendous progress and success in this field does not limit the research directions, but on the contrary, widens it. In the theoretical frontier, in the last couple of years alone, several new and interesting facets have emerged in this field which include port based quantum teleportation [20–23], fidelity enhancement of noisy QT using quantum switch [24–27], teleportation involving multiple parties [28–31], multiround quantum teleportation using weak measurements [32], fidelity deviation in QT [33].

Among these various avenues, let us briefly discuss and elaborate on the importance of the idea of fidelity deviation in QT. Typically, the performance of QT is measured by the average fidelity. However, such a mean-based characterization has some limitations since it cannot capture the fluctuations in fidelity with the various choices of inputs from the ensemble of states that are supplied for teleportation. For example, fluctuations become very important in situations where teleportation is used as an intermediate step in a quantum information processing task involving quantum gates. Since the performance of quantum gates depends on the fluctuations of its input (that reaches the gate via QT) [34, 35], the fidelity deviation must be taken into account on top of average fidelity for characterizing the quality of QT. Noting its importance, several works have been carried out in investigating the role of fidelity deviation in QT [36–39]. However, all of these studies is limited to discrete variable systems.

Continuous variable (CV) systems offer some distinct ad-

vantages over their discrete counterparts whereby they can overcome certain difficulties, like Bell-basis indistinguishability via linear optics [40]. Furthermore, they can be prepared with near perfect efficiency by using nonlinear interaction of a crystal with laser, and the only imperfection can arise due to the varying intensity of laser light, resulting in a low squeezing parameter [41], thereby making them potential systems for implementing quantum information processing tasks. Among the set of CV systems, Gaussian states hold a privileged position owing to their mathematical simplicity and experimental realizability [42–45].

Notably, it was in the Gaussian domain that the idea of CV teleportation was first conceptualized by Vaidman, Braunstein and Kimble (referred to as the VBK protocol) [46, 47]. From its inception, several directions have been explored in CV QT by varying the one-shot fidelity [48, 49] and the average fidelity [50]. It includes the extension of the protocol to non-Gaussian regimes, exhibiting that photon subtracted (PS) states can outperform the two mode squeezed vacuum (TMSV) state according to the average fidelity [48, 51–56], incorporating noise [49, 50, 57, 58], constructing CV QT networks [59–61], understanding the relationship between measures of quantum correlations and the fidelity [62–69] (a problem which is considerably well understood in the discrete case [2, 3]) and many more. To show quantum advantage, the classical threshold for the coherent state is shown to be at most half and quantum resources are known to beat the optimum measure-prepare strategy for moderate to high values of the squeezing parameter (see Fig. 1). For a more detailed review of the literature, see [70].

In this work, we focus on two independent aspects of CV quantum teleportation. On one hand, our work focuses on assessing the quality of the protocol with respect to the variation in input energy. Specifically, we consider input states coming from different energy distributions - uniform distribution having a finite threshold in the maximum permissible energy to avoid divergence and Gaussian distributions characterized by a specific standard deviation. For example, we study

how the average fidelity scales with different input distributions and examine the regimes at which quantum advantage is apparent, since the classical bound also varies for different energy constraints. In this new paradigm, we also compute the entanglement-free (measure-prepare) bound on QT to show where quantum advantage is manifested. On the other hand, we introduce the concept of the second moment of the fidelity statistics, the fidelity deviation, in CV systems which quantifies how well a given resource aids in the teleportation of different states coming from a given ensemble. A lower value of the fidelity deviation indicates that the resource is capable of transferring various input states with fidelities very close to the average fidelity. This is essential, since even if the average fidelity is high, a large deviation means that some states might still be teleported with suboptimal fidelity.

Our aim here is to determine the performance of QT by examining both the average fidelity and fidelity deviation and classify the CV resource states, both Gaussian TMSV as well as photon added and subtracted states according to their performances. Specifically, we report that contrary to the known results, TMSV states turn out to be better suited for CV QT than the PS states in many situations in presence or absence of noise. The investigations are carried out for different input states, coherent, squeezed, and squeezed coherent states when entangled channels are shared. In a noisy regime, we show that noise in measurement can be circumvented by a moderate amount of noise in channels, which we refer to as a constructive effect irrespective of the input energies. Moreover, we observe that noise in measurement at the sender's end has adverse effects on the quality of CV QT in terms of the average fidelity and its deviation compared to the noise in the channels. However, both the noise models have more detrimental effects on non-Gaussian states than the Gaussian ones, thereby establishing the TMSV state as a suitable channel for teleportation in presence of high input energy.

The paper is organized as follows. Before presenting the results, we introduce the monitors which can assess the performance of QT, the role of input energy in the performance and describe briefly the classical limit in each situation (Sec. II). The trends of average fidelity and fidelity deviation for noiseless CV teleportation with respect to different inputs and resource states are presented in Sec. III. The hierarchies among states according to the fidelity deviation are studied in Sec. IV for the noiseless case. In Sec. V, we investigate the effects of noise on the performance of CV QT by considering the average fidelity while the behavior of fidelity deviation in presence of noise is discussed in Sec. VI. Finally, we make the concluding remarks in Sec. VII.

II. REGULARIZED FIGURES OF MERIT

Continuous variable systems are characterized by canonically conjugate observables, say X and P , possessing a continuous spectrum. The system Hamiltonian for N such pairs,

each of which corresponds to a different mode, reads as

$$H = \frac{1}{2} \sum_{k=1}^N (X_k^2 + P_k^2) = \sum_{k=1}^N a_k^\dagger a_k + \frac{N}{2}, \quad (1)$$

where k denotes the mode, while a_k and a_k^\dagger represent the photon annihilation and creation operator respectively with

$$a_k = \frac{X_k + iP_k}{\sqrt{2}}, \text{ and } a_k^\dagger = \frac{X_k - iP_k}{\sqrt{2}}, \quad (2)$$

where $i = \sqrt{-1}$. When a single mode state, $|\psi_{in}\rangle$, has to be teleported through a CV channel, the overlap between the output state after implementing the protocol, ρ_{out} , and the input state $|\psi_{in}\rangle$, referred to as the fidelity $f(|\psi_{in}\rangle) = \langle \psi_{in} | \rho_{out} | \psi_{in} \rangle$ measures the efficacy of the protocol. When the standard CV teleportation scheme is followed [47], the fidelity can be expressed as

$$f_{|\psi_{in}\rangle} = \frac{1}{\pi} \int d^2\alpha \chi_{in}(-\alpha) \chi_{out}(\alpha), \quad (3)$$

where $\chi_\rho(\alpha) = \text{tr}(\rho D(\alpha))$, $D(\alpha)$ being the displacement operator, and $\chi_\rho(\alpha)$ is the characteristic function of the single-mode state ρ .

In our work, we primarily choose $|\psi_{in}\rangle$ to be a single mode pure Gaussian state [71]. Recall, the most general single mode pure Gaussian states are the squeezed-coherent states [43], and therefore, most generally,

$$|\psi_{in}\rangle \in \{S(\xi)D(\beta)|0\rangle\} \forall \xi, \beta \in \mathbb{C}, \quad (4)$$

where $S(\xi) = \epsilon e^{i\theta}$ represents the single mode squeezing operator with $|\xi| = \epsilon$ being the squeezing strength while θ denotes the squeezing angle. Here $\beta = b e^{i\phi}$ is the displacement parameter. Choosing $|\psi_{in}\rangle$ uniformly from the above ensemble is unphysical since it leads to divergent energies, which can be noted from the average energy of $|\psi_{in}\rangle$,

$$E_{|\psi_{in}\rangle} = \langle \psi_{in} | H | \psi_{in} \rangle = b^2 + \sinh^2 \epsilon. \quad (5)$$

This divergence can be prevented by imposing a distribution $p(\beta, \xi)$ with $\frac{1}{\mathcal{N}} \int p(\beta, \xi) d^2\beta d^2\xi = 1$ on the choice of $|\psi_{in}\rangle$ such that the average energy for the distribution of input states

$$E_{avg} = \frac{1}{\mathcal{N}} \int p(\beta, \xi) E_{|\psi_{in}\rangle} d^2\beta d^2\xi < \infty. \quad (6)$$

Endowed with this prescription for taming the divergences, we classify the performance of CV quantum teleportation using the first two moments of fidelity, referred to as the average fidelity [57], given by

$$\mathcal{F} = \frac{1}{\mathcal{N}} \int p(\beta, \xi) f_{|\psi_{in}\rangle} d|\psi_{in}\rangle, \quad (7)$$

with $\mathcal{N} = \int p(\beta, \xi) d|\psi_{in}\rangle$ while the corresponding fidelity deviation [33] reads as

$$\Delta\mathcal{F} = \sqrt{\langle f_{|\psi_{in}\rangle}^2 \rangle - \mathcal{F}^2}, \quad (8)$$

where $\langle f_{|\psi_{in}\rangle}^2 \rangle = \frac{1}{\mathcal{N}} \int p(\beta, \xi) f_{|\psi_{in}\rangle}^2 d|\psi_{in}\rangle$. Notice that in the discrete case, the measure " $d|\psi_{in}\rangle$ " implies the entire space of

inputs chosen uniformly from the Hilbert space of the relevant dimension, i.e., $p(\beta, \xi)$ is an uniform distribution. Here in CV systems, we choose the measure $d|\psi_{in}\rangle$ with reasonable cut-offs as mentioned before, making the average energy of the input ensemble finite. This allows us to construct regularized versions of average fidelity and fidelity deviation that are free from typical divergences arising due to infinite dimensional systems.

In our analysis, we consider two different realizations of $p(\beta, \xi)$, one with a finite cut-off in energy which we call the constrained uniform distribution, and the other with a Gaussian suppression, respectively given by

$$p_C(\beta, \xi) = \begin{cases} \text{constant}, & E_{|\psi_{in}\rangle} \leq \mathcal{E} \\ 0, & E_{|\psi_{in}\rangle} > \mathcal{E} \end{cases}, \quad (9)$$

$$p_G(\beta, \xi) = e^{-\frac{b^2}{\sigma_s^2}} e^{-\frac{\epsilon^2}{\sigma_c^2}}. \quad (10)$$

Both of these distributions rectify the divergent issues. From Eq. (5), the condition in Eq. (9) can be rewritten as $b^2 + \sinh^2 \epsilon \leq \mathcal{E}$. In this case, the average fidelity can be modified as

$$\mathcal{F} = \frac{1}{\mathcal{N}} \int_{\epsilon=0}^L \int_{\theta=0}^{2\pi} \int_{b=0}^{\sqrt{\sinh^2 L - \sinh^2 \epsilon}} \int_{\phi=0}^{2\pi} f_{|\psi_{in}\rangle} d|\psi_{in}\rangle, \quad (11)$$

where $d|\psi_{in}\rangle = b \epsilon d\epsilon d\theta db d\phi$ and the integral over the displacement parameter b runs from zero to the part of the total energy not carried by the squeezing. We assume that the total energy is given by $\sinh^2 L = \mathcal{E}$, where L is the maximum value that the squeezing parameter of the state, ϵ , can possess. The integration measure in Eq. (11) becomes $d|\psi_{in}\rangle = d^2\xi = 2\pi\epsilon d\epsilon$ for the squeezed state, whereas for the coherent state, it is $d|\psi_{in}\rangle = d^2\beta = b db d\phi$. Since it is hard by state of the art experiments to achieve squeezing beyond $r = 1.6$ [72], we accordingly fix the energy threshold for the squeezed state as $L_\xi = 1.6$ such that $\sinh^2 \epsilon \leq \sinh^2 L_\xi$. In order to facilitate comparison, we also consider the energy cut-off for the coherent state to be the same, due to which $|L_\beta|^2 = \sinh^2 L_\xi$ even though technically, it can possess relatively high energy.

For the Gaussian distribution of squeezed-coherent states, the integrals for computing average fidelity and fidelity deviation get simplified forms since $p_G(\beta, \xi)$ acts independently on the coherent and squeezed sectors owing to its product structure. Note that such simplification is not possible with uniform distribution having energy thresholds. Using Eq. (7) with the condition in Eq. (10), the average fidelity for teleporting squeezed-coherent states can be computed as

$$\mathcal{F} = \frac{1}{\mathcal{N}} \int_{\epsilon=0}^{\infty} \int_{\theta=0}^{2\pi} \int_{b=0}^{\infty} \int_{\phi=0}^{2\pi} \times f_{|\psi_{in}\rangle} \exp\left(-\frac{\epsilon^2}{\sigma_s^2}\right) \exp\left(-\frac{b^2}{\sigma_c^2}\right) d|\psi_{in}\rangle, \quad (12)$$

where $\mathcal{N} = (\pi\sigma_s)(\pi\sigma_c)$, with σ_s and σ_c being the standard deviations corresponding to the input squeezing and the displacement parameters respectively.

Using Eq. (6), the average input energy is computed to be $(\sigma_c + \frac{1}{2}e^{\sigma_s} \sqrt{\pi\sigma_s} \text{Erf}(\sqrt{\sigma_s}))$, where the first term represents the average energy for input coherent state and the second term corresponds to the average energy for input squeezed state individually. Here Erf is the error function given by $\text{Erf}(x) = \frac{2}{\sqrt{\pi}} \int_0^x e^{-t^2} dt$. Since the average energy depends both on σ_s and σ_c and increases with them, we take the range of σ_s and σ_c up to 5.0 and 10.0 respectively in order to capture all possible prime features that the figures of merit can exhibit, with respect to the average input energy. Before presenting all results, both in the noiseless and noisy scenarios, let us briefly discuss the classical limit for CV quantum teleportation which is essential to estimate any quantum advantage.

A. The classical limit

In any quantum information protocol, it is necessary to define a classical threshold which quantifies the performance of the optimal classical routine for the task. If the figure of merit for the quantum protocol exceeds the classical limit, we can claim with certainty that quantum benefit is obtained. In quantum teleportation with the discrete qubit formalism, an average fidelity beyond $\mathcal{F} = 2/3$ indicates the presence of entanglement, thereby obtaining quantum advantage [2, 7, 73].

In CV teleportation, when the input states, say coherent states are sampled from a Gaussian distribution with standard deviation λ^{-1} [74], the optimal fidelity achievable through classical measure-prepare strategy is known to be $F_{class}^{coh} \leq (1 + \lambda)/(2 + \lambda)$ [75]. If the distribution becomes completely flat, i.e. $\lambda = 0$, it reduces to $F_{class}^{coh} \leq 0.5$. Therefore, for states sampled from an infinitely flat distribution of energies, any fidelity above 0.5 guarantees quantum advantage. However, if the standard deviation of a Gaussian distribution is finite ($\lambda > 0$), or there exists a uniform distribution which contains states up to a particular energy only (as in Eq. (9)), the classical threshold increases beyond the aforementioned value. It can be intuitively understood since it is easier for the concerned parties to replicate the input state through a measure-prepare strategy when the states are drawn from a limited energy distribution [75]. Hence, the classical bound on the average fidelity depends on average input energy and decreases with the decrease in the spread of input energy. Specifically, for a given distribution with a finite energy, we need to determine the corresponding fidelity which is achievable in absence of entanglement.

Similarly, the optimal classical bound on the teleportation of squeezed states is not uniquely determined and is no longer bounded by 0.5 [76]. In Ref. [77], it was demonstrated that the classical protocol for sending squeezed states with a flatly distributed energy up to a maximum value can go higher than 0.9. Similarly, for pure input squeezed states, a fidelity higher than 81.5% is necessary to obtain quantum advantage, when the states belong to an infinite ensemble of uniformly distributed energy [78].

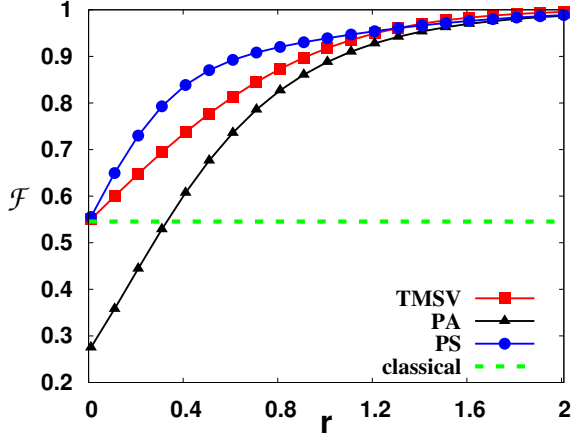


FIG. 1. The average teleportation fidelity, \mathcal{F} (ordinate) of coherent states drawn from a Gaussian ensemble of standard deviation, $\sigma = 5.0$ against the squeezing of the entangled resource states, r (abscissa). Squares, circles, and triangles represent the TMSV, photon added (PA) and photon subtracted (PS) states as channels. The classical bound on the average fidelity is shown in dashed lines. It is interesting to observe whether such hierarchies among CV states change with different input distributions like uniform distribution with energy threshold. Both the axes are dimensionless.

III. CHARACTERIZING NOISELESS CV TELEPORTATION VIA AVERAGE FIDELITY AND FIDELITY DEVIATION

Before presenting the results in the absence of any kind of noise, let us specify the resource and input states considered here.

Resources. In our analysis, the shared resource state used are squeezed Bell-like states which read as

$$|\Phi\rangle = \hat{S}_{12}(\zeta)(\cos\delta|00\rangle + e^{i\eta}\sin\delta|11\rangle), \quad (13)$$

where $\hat{S}_{12}(\zeta) = e^{-\zeta a_1^\dagger a_2^\dagger + \zeta^* a_1 a_2}$ is the two-mode squeezing unitary operator with $\zeta = r e^{i\gamma}$. It can be reduced to different well-known Gaussian and non-Gaussian states – for $\delta = 0$, it represents the two-mode squeezed vacuum state; $\delta = \arccos[(\cosh 2r)^{-1/2} \sinh r]$ and $\eta = \gamma - \pi$ gives the two mode photon added squeezed vacuum state (PA); and by choosing $\delta = \arccos[(\cosh 2r)^{-1/2} \cosh r]$ and $\eta = \gamma - \pi$, we obtain the two mode photon subtracted (PS) state, where the last two are the non-Gaussian states. Note that a single photon is added (subtracted) in both the modes to create photon added (subtracted) states. In this work, comparative analysis of utility in using all three quantum channels between the sender and the receiver is performed.

Inputs. Three paradigmatic input states, namely the coherent state having displacement parameter $\beta = b e^{i\phi}$ given by $|\psi\rangle_c = \hat{D}(\beta)|0\rangle$, the squeezed state with squeezing parameter ξ i.e. $|\psi\rangle_s = \hat{S}(\xi)|0\rangle$ and the squeezed-coherent state, $|\psi\rangle_{sc} = \hat{S}(\xi)\hat{D}(\beta)|0\rangle$ are considered for investigation. Here, $\hat{D}(\beta) = \exp(\beta\hat{a}^\dagger - \beta^*\hat{a})$ is the displacement operator and $\xi = \epsilon e^{i\theta}$. Notice that by examining the behavior of

squeezed coherent states as inputs in QT, the role of other input states on QT can be derived. The analytical expression of the fidelity f for teleporting a squeezed-coherent state using squeezed Bell state as a resource is given by [79]

$$f_{|\psi\rangle_{sc}} = \frac{4}{\sqrt{\Lambda_1\Lambda_2}} e^{\frac{\omega_1^2}{\Lambda_1} - \frac{\omega_2^2}{\Lambda_2}} \left[1 + e^{-2r} \sin\delta (\Delta_2 \cos\delta - \Delta_1 \sin\delta) \left\{ \frac{1}{\Lambda_1} \left(1 + \frac{2\omega_1^2}{\Lambda_1} \right) + \frac{1}{\Lambda_2} \left(1 - \frac{2\omega_2^2}{\Lambda_2} \right) \right\} + \frac{1}{4} e^{-4r} \Delta_2^2 \sin^2\delta \left(\frac{1}{\Lambda_1^2} \left\{ 3 + \frac{12\omega_1^2}{\Lambda_1} + \frac{4\omega_1^4}{\Lambda_1^2} \right\} + \frac{1}{\Lambda_2^2} \left\{ 3 - \frac{12\omega_2^2}{\Lambda_2} + \frac{4\omega_2^4}{\Lambda_2^2} \right\} + \frac{2}{\Lambda_1\Lambda_2} \left\{ 1 + \frac{2\omega_1^2}{\Lambda_1} - \frac{2\omega_2^2}{\Lambda_2} - \frac{4\omega_1^2\omega_2^2}{\Lambda_1\Lambda_2} \right\} \right) \right], \quad (14)$$

where the parameters $\Delta_1, \Delta_2, \Lambda_1, \Lambda_2, \omega_1^2$ and ω_2^2 take the form as

$$\begin{aligned} \Delta_1 &= (1 + e^{4r}) + 2(1 - e^{4r})g + (1 + e^{4r})g^2, \\ \Delta_2 &= (12e^{4r}) + 2(1 + e^{4r})g + (1 - e^{4r})g^2, \\ \Lambda_1 &= e^{-2r}\Lambda_1 + 2e^{2\epsilon}(1 + g^2), \\ \Lambda_2 &= e^{-2r}\Lambda_1 + 2e^{-2\epsilon}(1 + g^2), \\ \omega_1^2 &= (1 - g^2)(\beta - \beta^*)^2, \\ \omega_2^2 &= (1 - g^2)(\beta + \beta^*)^2. \end{aligned} \quad (15)$$

Here $g \in (0, 1)$ is the gain factor involved in the measurement performed by the receiver [74]. Equipped with this fidelity expression, we compute the maximal average fidelity (\mathcal{F}) by optimizing over g and its corresponding fidelity deviation ($\Delta\mathcal{F}$) both for the constrained uniform and Gaussian distributions of input states using Eqs. (7) - (10).

A. Trends of average fidelity and fidelity deviation with resource squeezing

Let us first investigate the response of the quality factors for teleportation with respect to the squeezing parameter, r of the shared resource state. For all the three shared states considered here, namely the TMSV, PA and the PS states, the average fidelity increases monotonically with r for both constrained uniform and Gaussian distribution of input states (see Fig. 1). This is intuitively satisfactory since the EPR correlation increases with an increase of r and the VBK protocol of teleportation uses EPR correlations as resource. We will repeatedly return to these enhancement of features on increasing r in situations where the average fidelity fails to beat the classical limit. Instead of discussing the behavior of average fidelity which is studied and known with r , let us concentrate on the fidelity deviation with respect to r for different types of input states as well as resources and for a fixed average energy of the input distribution (see Fig. 2). We categorize the trends according to the input states in the following manner.

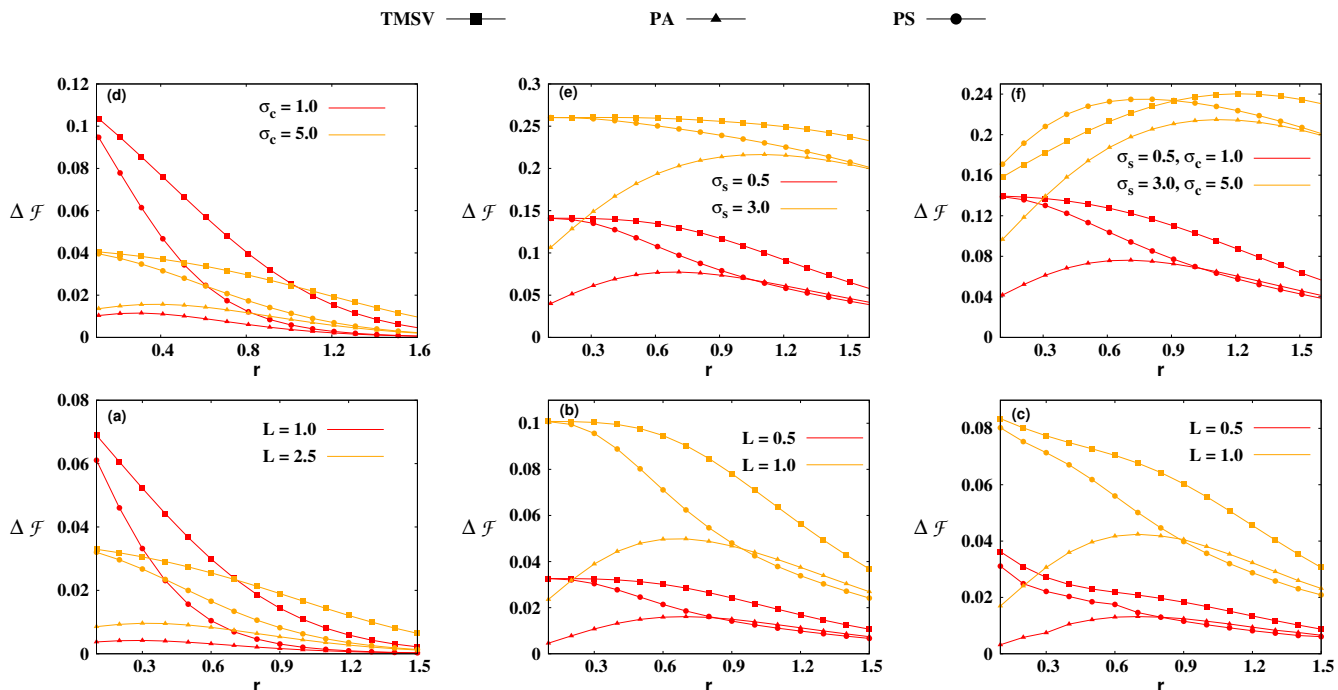


FIG. 2. The variation of fidelity deviation, $\Delta\mathcal{F}$ (vertical axis) vs. squeezing of the shared channels, r (horizontal axis) for uniform distribution (lower panel) and Gaussian distribution (upper panel) of different input states in the case of both Gaussian and non-Gaussian resource states. Symbols used for shared channels are same as in Fig. 1. (Lower panel) Plot of $\Delta\mathcal{F}$ for (a) coherent input states with energy cut-off $L = 1.0$ (dark red) and $L = 2.5$ (gray yellow), (b) squeezed input states with $L = 0.5$ (dark red) and $L = 1.0$ (gray yellow) and (c) squeezed-coherent input states with the same energy threshold specifications as in (b). (Upper panel) $\Delta\mathcal{F}$ for different inputs, (d) coherent states with $\sigma_c = 1.0$ (dark red) and $\sigma_c = 5.0$ (gray yellow), (e) squeezed states with $\sigma_s = 0.5$ (dark red) and $\sigma_s = 3.0$ (gray yellow) and (f) squeezed-coherent states having $\sigma_s = 0.5, \sigma_c = 1.0$ (dark red) and $\sigma_s = 3.0, \sigma_c = 5.0$ (gray yellow). All the axes are dimensionless.

Squeezed states: Unlike the average fidelity, a low values of fidelity deviation ensures good performance of the resource states. For input squeezed states, we observe that the photon added states provide the least deviation from the average fidelity for small resource squeezing, while the PS state accomplishes the task with minimum $\Delta\mathcal{F}$ for higher values of r . This is true when states are sampled both from the uniform (Fig. 2 (b)) as well as the Gaussian distribution (Fig. 2 (e)). On the other hand, $\Delta\mathcal{F}$ increases with the increase in input energy, i.e., with the increase of L and σ_s .

Coherent states: We observe the decreasing trends of $\Delta\mathcal{F}$ with the increase of r in the resource, irrespective of the resource state. Like in the previous case, PA states still provide the least deviation compared to PS or TMSV states although the PS states overtake it at a very high squeezing. Moreover, we find that unlike the squeezed states, there seems to be a complex relation between the squeezing in resource and energy threshold in inputs. In particular, $\Delta\mathcal{F}$ is low for ensembles with high energy up to a moderate value of r both for the shared TMSV and PS states although the magnitude of the squeezing required is more for the TMSV states than the PS states. For example, $\Delta\mathcal{F}_{L\beta=2.5} < \Delta\mathcal{F}_{L\beta=1.0}$ upto $r_{PS} \leq 0.4$ while the similar hierarchy exists for the shared TMSV

with a higher r , i.e., $\Delta\mathcal{F}_{L\beta=2.5} < \Delta\mathcal{F}_{L\beta=1.0}$ when $r_{TMSV} \leq 0.7$. Similar behavior is also observed for the Gaussian distribution (as shown in Figs. 2 (a) and (d)).

Squeezed-coherent states: The behavior of fidelity deviation with variation in resource squeezing for input squeezed-coherent states is similar to the other two inputs. The only significant difference is the disparity in $\Delta\mathcal{F}$ for uniform and Gaussian distribution at higher energies. For states chosen from a Gaussian assemblage, the PS state constitutes the protocol with the highest value of $\Delta\mathcal{F}$ for low squeezing strengths at high input energies. As r increases, its deviation falls below that of the Gaussian TMSV state (for $r \gtrsim 1.0$) but still cannot overcome the one that is furnished by the PA states as resource. However, for constrained uniform distribution, the PS states teleport with minimum $\Delta\mathcal{F}$ at moderate to high r in the resource.

B. Role of input energies in teleportation

As mentioned before, one of the main focus of this work is to find the effects of the energy threshold in the input ensem-

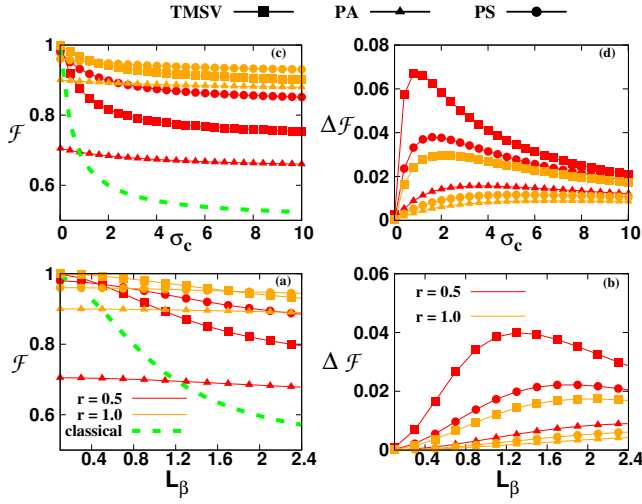


FIG. 3. Average fidelity ((a) and (c)) and fidelity deviation ((b) and (d)) (ordinate) with respect to energy threshold, L_β in uniform distribution (lower panel) and σ_c for Gaussian distribution (upper panel) (abscissa). Symbols for channels are same as in Fig. 1. In (a)-(d), inputs are taken to be coherent states having $r = 0.5$ (dark (red)) and 1.0 (gray (yellow)). All the axes are dimensionless.

ble on the average fidelity and its deviation. Specifically, we examine \mathcal{F} and $\Delta\mathcal{F}$ with the variation of L in the constrained uniform distribution and σ_s as well as σ_c of the Gaussian distribution.

Average fidelity: Let us illustrate the dependence of L , σ_s and σ_c on \mathcal{F} for a fixed resource squeezing r which is chosen to be moderate (for demonstration, we choose e.g. $r = 0.5$, and 1.0). We observe that the average fidelity decreases monotonically with an increase in the input cut-off L and with an increase in the standard deviation σ for a fixed value of r in the channel, irrespective of shared states and inputs as depicted in Figs. 3 and 4. It is possibly due to the fact that the performance of QT decreases with the increase of energy to be teleported, indicated by the greater value of $L(\sigma)$. Note, however, that a more involved picture emerges when inputs are drawn from the Gaussian distribution – the rate of decrements in \mathcal{F} with respect to σ_s is faster than that with σ_c (see Fig. 4). We observe that to transfer states with a high degree of squeezing or displacement, we require a highly squeezed resource state (containing high entanglement) to ensure that the protocol is successful. We also find that the TMSV states can furnish a higher value of \mathcal{F} for low energy Gaussian ensembles, with $\sigma \sim 0.1$ which depends also on the squeezing strength of the channel although PS states outperform over TMSV states in other ranges of input energies.

Fidelity deviation: As seen in case of the average fidelity, the increase of energy threshold in terms of increasing L (σ) creates an obstacle in the success of the QT process, due to increase of the fidelity deviation with energy, irrespective of the resource states and inputs, except for the

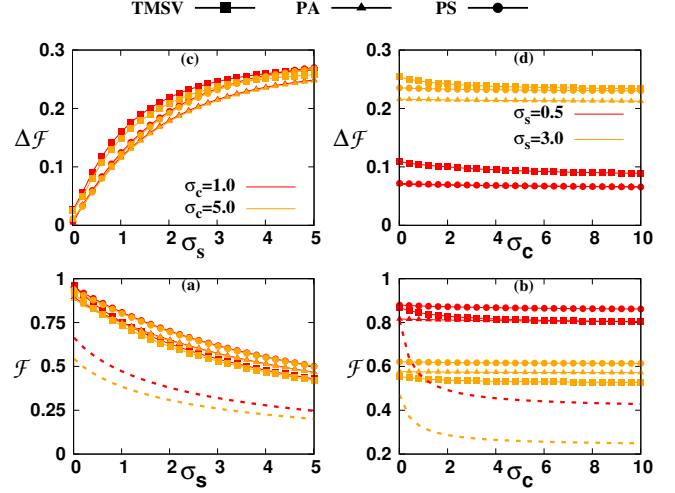


FIG. 4. Average fidelity (lower panel) and fidelity deviation (upper panel) (ordinate) against the standard deviations of squeezed-coherent input states, σ_s ((a) and (c)) and σ_c ((b) and (d)). Symbols are same as in Fig. 1 with resource squeezing $r = 1.0$. In (a) and (c), $\sigma_c = 1.0$ (dark (red)) and $\sigma_c = 5.0$ (gray (yellow)), while in (b) and (d), $\sigma_s = 0.5$ (in dark (red)) and $\sigma_s = 3.0$ (in gray (yellow)). The classical bounds on the average fidelity are shown in dashed line with respective colours. All the axes are dimensionless.

coherent states. In case of coherent states, $\Delta\mathcal{F}$ exhibits a *nonmonotonic* behavior with input-energy, i.e., there is a threshold value of L and σ_c up to which it increases and subsequently decreases after the criticality. Such nonmonotonicity can be eliminated by increasing r of the channel (see Figs. 3 (b) and (d)). E.g. considering the TMSV state as resource, the criticality shifts from $\sigma_c \sim 0.8$ ($L \sim 1.2$) to $\sigma_c \sim 2.0$ ($L \sim 2.0$) when the resource squeezing is increased from 0.5 to 1.0.

From the patterns of \mathcal{F} and $\Delta\mathcal{F}$, we can safely conclude that for a teleportation protocol to succeed with a high average fidelity such that states are transferred with small variance in the desired fidelity, resource states with a moderate to high degree of squeezing are preferred, thereby demonstrating inverse proportionality between \mathcal{F} and $\Delta\mathcal{F}$. In particular, by considering input squeezed states from Gaussian distribution, the resource squeezing required to teleport states increases with the corresponding standard deviation when the average fidelity is our major concern. On the other hand, in case of high average input energy, we need to make a compromise between the demand of high average fidelity and the low fidelity deviation in order to justify the quality of a resource state.

Quantum vs. Entanglement-free protocol. Let us make a comparison between quantum protocols, which uses entangled channels, and entanglement-free (setting $r = 0.0$) ones in terms of the average fidelity. In this study, the squeezed or coherent states as inputs behave similarly compared to the squeezed coherent states. For very low values of the standard deviations, e.g. $\sigma_s \sim 0.2$ or $\sigma_c \sim 0.1$, or low input energy upper bound, $L \leq 0.1$, with squeezed or coherent states as inputs, the entanglement-free protocol performs equally well

as the entangled one. This may be due to the fact that for such low input energies, the unentangled protocol itself can furnish a very high average fidelity. As the energy of the input ensemble increases, the entanglement-based protocols win even with low values of the resource squeezing. However, such energy thresholds are not present in case of squeezed-coherent states as input, i.e., quantum routine outperforms the classical one in the entire range of both standard deviations as shown in Fig. 4. Comparing resource states, we notice that for a uniform distribution in inputs, the TMSV and PS states always manage to beat the measure-prepare strategy while PA state can furnish quantum advantage only when the input energy is very high and the resource squeezing is substantial, say, $r \geq 1.0$.

IV. RESOURCES HIERARCHIES VIA FIDELITY DEVIATION

In this section, we highlight situations where the average fidelity alone cannot completely characterize the performance in teleportation by various resources. Specifically, we point out instances where resource states can be classified from the non-trivial variations obtained in fidelity deviation. Moreover, our analysis reveals that several parameters like the squeezing of the resource, distribution of input states, and energy content play an important role in the performance of QT.

1. Varying resource squeezing: Advantages of non-Gaussianity

With respect to average fidelity alone, there is clear hierarchy of resource states with the PS being the best, closely followed by TMSV, while the photon-added states turn out to be the worst, failing to beat the classical limit in some cases. Let us now show that the ranking gets more involved if we take into account both the moments of the fidelity statistics.

When the input states are chosen to be squeezed or coherent states, for both constrained uniform and Gaussian distributions, we get qualitatively similar behavior of fidelity deviation. The TMSV state shows the largest deviation among the three shared states. Therefore, for low r , PS is the best resource for quantum teleportation, since it not only possesses the highest average fidelity but also very low deviation, see Fig. 3. For high values of r , the average fidelity for all the resource states grows, and become almost identical and therefore, the classification of resource states is entirely dictated by the fidelity deviation. In this high r limit, the deviation for PA and PS also become nearly equal while TMSV possesses a visibly larger deviation compared to these two. Therefore, here PA and PS become the better resource for quantum teleportation while TMSV turn out to be the worst. This feature also points out the role of non-Gaussianity in QT over Gaussian resources, especially for large squeezing.

For squeezed coherent inputs, things become more involved and we sometime get different responses for constrained uniform and Gaussian distributions. However, note that for low average energies of the input, it mimics a pattern similar to the previous cases. Things become interesting when relatively

large values of input energies are considered. For example, for the Gaussian distribution, the PS has a larger deviation compared to the TMSV state for a range of relatively low r values. This implies that for that range of r values, we have to compare between two resources for which $\mathcal{F}_1 > \mathcal{F}_2$ and also $\Delta\mathcal{F}_1 > \Delta\mathcal{F}_2$ are satisfied, see Fig. 2. Such a comparison of resources is not straight forward and depends on the sensitivity requirements in deviation in a given context, see [38].

2. Varying input energies

TMSV and PS as channels. First of all, TMSV and PS states can always beat the entanglement-free protocol provided that the squeezing is not too low and the input energy is moderately high. We observe that at a fixed squeezing strength of the resource states, the photon subtracted state accounts for a higher average fidelity than that of the TMSV state, when the input ensemble has a squeezing cut-off or standard deviation over a certain value, viz. $L \gtrsim 0.8$ while the opposite hierarchy occurs in other situations. For example, for squeezed and coherent states as inputs belonging to a Gaussian ensemble up to a certain value of standard deviation, e.g. $\sigma_s \leq 0.2$ and $\sigma_c \leq 1.2$ (for $r = 1.0$), the shared TMSV state between the sender and the receiver performs better than the others in terms of the average fidelity. Notice that such a ranking among states is not possible unless both fidelity and its deviation are taken in to account.

Photon added states. The fidelity deviation for the photon added state is very low, especially when we consider its variation with respect to L , and for a high value of r . The PA state, however, is not a suitable resource for QT, since it can only outperform the entanglement-free protocol once the squeezing is substantial.

The fidelity deviation helps removing the degeneracy among resource states in terms of being the optimal one in the teleportation protocol. We observe that at high resource squeezing, according to \mathcal{F} , the non-Gaussian resources are always favorable over the TMSV one. However, introducing the fidelity deviation in picture, we find that only for high energy ensembles, the PS state offers the lower $\Delta\mathcal{F}$ along with high \mathcal{F} , thereby making it suitable for the QT purpose. Furthermore, at very low input energies, the average fidelity of the TMSV state is the highest among all states and the fidelity deviation, although higher than the non-Gaussian resources, is still very low ($O(10^{-2})$), thereby making it a reasonable resource as well. In the intermediate regimes, there is a competition between the high average fidelity offered by the PS state and low fidelity deviation by the PA state although again the PS state is favourable due to high average fidelity leading to quantum advantage. The above discussion also manifests that although non-Gaussian resources can help to improve the teleportation protocol, the resource state must be chosen wisely, and also according to the input energy.

V. NOISY CV TELEPORTATION

Upto now, the investigations are carried out with the assumption that there is no noise in the preparation of resources or in the measurement process. Typically, imperfections are inevitable during the realization of these protocols in laboratories. In our analysis, we consider two main sources of noise - one occurring in the state itself, due to losses in the fiber through which the modes of the entangled resource are transmitted to the concerned parties, while the other one arises due to imperfect Bell measurements performed at the sender's node.

The noisy channel quantified by $\tau = \gamma t$ is proportional to the fiber propagation length, where γ is the mode damping rate [57, 79], and the fibre loss factor is also associated with the interaction with a Gaussian bath of mean photon number n_{th} which is taken to be zero in our work [79]. On the other hand, the imperfection in Bell measurement is considered by incorporating photon losses during the procedure which is modelled with the help of a beam splitter of transmittivity \mathcal{T} and reflectivity \mathcal{R} . A non-zero value of \mathcal{R} indicates finite losses in measurement [57]. In the presence of the imperfections mentioned above, the expression of the one-shot fidelity for squeezed-coherent states can be written as

$$f'_{|\psi\rangle_{sc}} = \frac{4}{\sqrt{\Lambda_1 \Lambda_2}} e^{\frac{\omega_1^2}{\Lambda_1} - \frac{\omega_2^2}{\Lambda_2}} \left[1 + e^{-2r-\tau} \sin \delta \times \right. \\ \left. (\Delta_2 \cos \delta - \Delta_1 \sin \delta) \left\{ \frac{1}{\Lambda_1} \left(1 + \frac{2\omega_1^2}{\Lambda_1} \right) + \frac{1}{\Lambda_2} \left(1 - \frac{2\omega_2^2}{\Lambda_2} \right) \right\} \right. \\ \left. + \frac{1}{4} e^{-4r-2\tau} \Delta_2^2 \sin^2 \delta \left(\frac{1}{\Lambda_1^2} \left\{ 3 + \frac{12\omega_1^2}{\Lambda_1} + \frac{4\omega_1^4}{\Lambda_1^2} \right\} \right. \right. \\ \left. \left. + \frac{1}{\Lambda_2^2} \left\{ 3 - \frac{12\omega_2^2}{\Lambda_2} + \frac{4\omega_2^4}{\Lambda_2^2} \right\} \right. \right. \\ \left. \left. + \frac{2}{\Lambda_1 \Lambda_2} \left\{ 1 + \frac{2\omega_1^2}{\Lambda_1} - \frac{2\omega_2^2}{\Lambda_2} - \frac{4\omega_1^2 \omega_2^2}{\Lambda_1 \Lambda_2} \right\} \right) \right], \quad (16)$$

where

$$\begin{aligned} \Delta_1 &= (1 + e^{4r}) + 2e^{\tau/2}(1 - e^{4r})\tilde{g} + e^\tau(1 + e^{4r})\tilde{g}^2, \\ \Delta_2 &= (12e^{4r}) + 2e^{\tau/2}(1 + e^{4r})\tilde{g} + e^\tau(1 - e^{4r})\tilde{g}^2, \\ \Lambda_1 &= e^{-2r-\tau}\Lambda_1 + 2e^{2\epsilon}(1 + \tilde{g}^2) + 4\Gamma, \\ \Lambda_2 &= e^{-2r-\tau}\Lambda_1 + 2e^{-2\epsilon}(1 + \tilde{g}^2) + 4\Gamma, \\ \omega_1^2 &= (1 - \tilde{g}^2)(\beta - \beta^*)^2, \\ \omega_2^2 &= (1 - \tilde{g}^2)(\beta + \beta^*)^2, \end{aligned} \quad (17)$$

with $\tilde{g} = g\mathcal{T}$ and $\Gamma = \frac{1}{2}(1 - e^{-\tau}) + g^2\mathcal{R}^2$ [79]. In presence of both the noises, the average fidelity and the fidelity deviation are calculated after optimizing over g . To study the effects of noise on QT, the moments of fidelity are studied with respect to a single noise parameter, while maintaining the other at a fixed value, for different regimes of resource squeezing and input energy. Moreover, to discuss the results systematically, our findings for the constrained uniform and Gaussian distribution of inputs are presented separately.

A. Average fidelity with constrained uniform input distribution: Gaussian resources are better

Let us first consider the variation of the average fidelity \mathcal{F} with the measurement noise \mathcal{R} , for fixed values of the noise in channels, τ . As expected, the average fidelity decreases with an increase in the magnitude of \mathcal{R} , which is illustrated in the lower panels of Fig. 5. However, it can be increased if the resource squeezing is high or the input energy is low. Contrary to the noiseless scenario, the PS state provides the highest \mathcal{F} only for high energy input ensembles ($L_\xi = 1.0$) with low resource squeezing strengths and low noise limits up to $\mathcal{R}, \tau = 0.1$. Otherwise, when the states to be teleported are of high energy and the resource squeezing is also sufficient, \mathcal{F} for the Gaussian TMSV state is slightly higher than that of the PS state, thereby indicating its robustness against noise and also proving its appropriateness for noisy CV teleportation.

1. Counteracting one noise with the other - a constructive effect

Let us report here an interesting feature when different values of the resource squeezing are considered. By varying \mathcal{R} , one would expect the average fidelity to be low for higher values of τ , i.e., in presence of both the noises. This is indeed the case but not over the entire range of \mathcal{R} . We observe that there exists a region in \mathcal{R} where \mathcal{F} is higher in presence of resource noise, say $\tau = 0.3$ than that of the scenario without noise in resources, i.e. with $\tau = 0$. This can be interpreted as if the effect of one kind of noise is countered by the other one, thereby exhibiting a *constructive phenomenon* which is more pronounced in case of coherent inputs (see Fig. 5). It may also indicate that when the resource is affected by ineffective propagation, the protocol may not be the optimal even with a properly tuned gain parameter g . The point of crossover depends on the resource squeezing as well as on the energy of the input state. Comparing Fig. 5 (a) with (b) and (c), we realize that the constructive effect is more visible for non-Gaussian states compared to the Gaussian ones. Notice that the advantage is counted only when \mathcal{F} obtained in a noisy scenario is higher than the entanglement-free protocol without noise which we will discuss later.

The effects of noise on the average fidelity is also distinctive for different classes of input states. In particular, \mathcal{F} for the squeezed-coherent states ($\mathcal{F} \geq 0.4$) is much lower than that of the squeezed and coherent inputs ($\mathcal{F} \geq 0.7$), especially for high ensemble energies, which is not the case in the noiseless scenario. Moreover, the average fidelity decreases at a much faster rate for the PS and PA states, which indicates that the impact of noise is more on non Gaussian states in comparison with TMSV state having moderate squeezing. Furthermore, the difference between \mathcal{F} at higher and lower values of τ is least for the PA state, ~ 0.005 , but significantly more for the TMSV and PS states, ~ 0.01 .

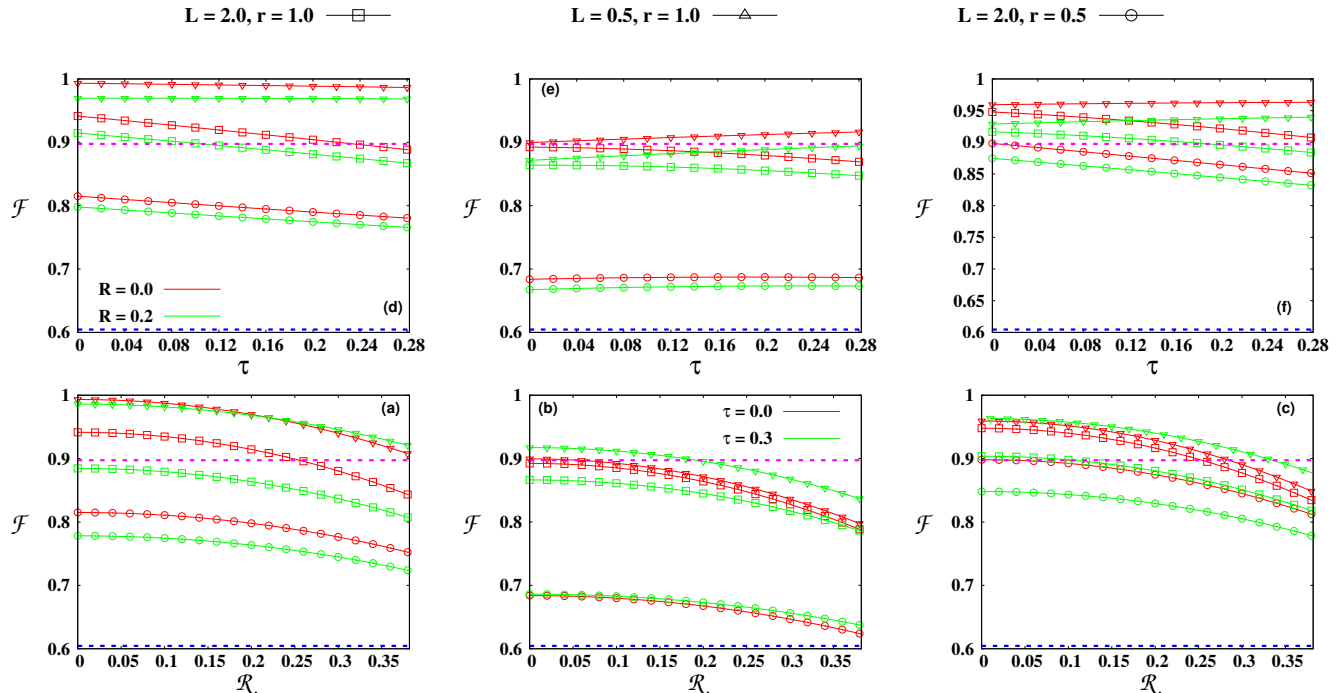


FIG. 5. Average fidelity (along ordinate) vs. noise parameters, \mathcal{R} (lower panel) and τ (upper panel) (along abscissa) for TMSV (a) and (d), PA (b) and (e), PS (c) and (f) resource states with coherent states as input. (Lower panel) \mathcal{R} is varied for fixed $L = 2.0, r = 1.0$ (hollow squares), $L = 0.5, r = 1.0$ (hollow triangles) and $L = 2.0, r = 0.5$ (hollow circles) at resource noise values $\tau = 0.0$ (dark red) and $\tau = 0.3$ (gray (green)). The classical bounds obtained by measure-prepare strategy are shown corresponding to $L = 0.5$ (dashed gray (pink)) and $L = 1.0$ (dashed dark (blue)). (Upper panel) When noise, τ in the channel varies, the measurement noise are fixed to $\mathcal{R} = 0.0$ (dark red) $\mathcal{R} = 0.2$ (gray (green)). All other specifications are same as the lower panel. All the axes are dimensionless.

2. Robustness against resource noise

Let us now fix a moderate amount of noise in measurement (e.g. we choose $\mathcal{R} = 0.0$, and 0.2) and study the dynamics of average fidelity by varying noise in the shared channel. First of all, no constructive effects with τ is seen by comparing $\mathcal{R} = 0$ and $\mathcal{R} = 0.2$ (see Fig. 5). However, the decrease in \mathcal{F} with increase of τ is much slower than the one observed by varying \mathcal{R} especially when the squeezing strength in resource is high, irrespective of Gaussian or non Gaussian resource states and inputs (comparing upper and lower panel of Fig. 5). It demonstrates the adverse effects of inefficient measurement on the protocol compared to noise in resource states. However, such detrimental impact can again be wiped out in presence of high squeezing in the shared channel.

3. Comparison with the unentangled protocol

The teleportation protocol with unentangled states (classical protocol) involves a measure-prepare routine, which evidently does not suffer from the noise models considered here. Therefore, it is justified to examine whether the noisy teleportation process can beat the noiseless classical one.

All the different scenarios have so far been compared keeping in mind the quantum advantage, i.e., the shared TMSV

states with coherent inputs to be teleported exhibits maximum robustness against both the noise models considered here. Moreover, as the input energy increases, the TMSV state can retain quantum advantage in presence of large amount of noise. For example, for $L = 0.5$, the TMSV state with $r = 1.0$ can outperform the unentangled protocol up to $\mathcal{R} \sim 0.16$, while the same resource can retain quantum advantage for $\mathcal{R} \leq 0.28$ with $L = 1.0$ in case of squeezed input states. The situation changes in case of the squeezed-coherent ensembles when the TMSV state can outperform the classical scheme only for low input energies and for higher values of L only up to small magnitudes of noise.

In case of photon added state, the regimes of quantum advantage are very limited especially for squeezed input states and for low input energy. Quantum advantage can only be found for low \mathcal{R} and τ . The PS state performs better than its photon added counterpart irrespective of inputs. Again, it performs best for coherent input states, always outperforming the classical measure-prepare routine for high input energy. For low L_β , it can furnish quantum advantage with sufficient squeezing ($r \geq 1$) unless \mathcal{R} and τ are too high while both for squeezed and squeezed-coherent input states, the entangled states win over the classical protocol with high squeezing and energy cut-offs when noise in the channel and measurements is low.

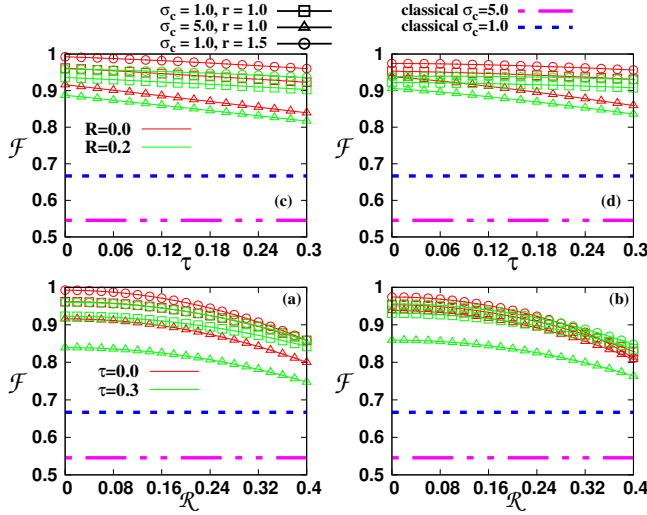


FIG. 6. Average fidelity (ordinate) with noise parameters, \mathcal{R} (lower panel) and τ (upper panel) (abscissa). Input states are chosen to be again coherent states drawn from a Gaussian distribution with TMSV (left panel) and PS (right panel) as resources. In all the panels, the standard deviation and resource squeezing are depicted as $\sigma_c = 1.0, r = 1.0$ (hollow squares), $\sigma_c = 5.0, r = 1.0$ (hollow triangles) and $\sigma_c = 1.0, r = 1.5$ (hollow circles). The classical threshold corresponding to $\sigma_c = 5.0$ is shown with dashed gray (pink) lines while dotted-dashed dark (blue) line represents $\sigma_c = 1.0$. All other specifications are same as in Fig. 5. All axes are dimensionless.

B. Effects of Gaussian input distribution on noisy teleportation

A similar examination is carried out when the input states are sampled from a Gaussian distribution. Unlike the constrained uniform distribution, all input states, squeezed, coherent and squeezed-coherent share more or less similar properties of average fidelity with respect to both noise parameters. So, we mainly discuss the behavior of average fidelity for input squeezed states and explicitly mention the corresponding situations for other input states whenever we come across any individual feature.

As already emphasized, we will only present those situations in which the performance of QT protocol is better than the prepare-measure strategy even in the presence of noise. Like in the uniform case, the quantum process always outperforms the classical one in case of teleporting input coherent states irrespective of all resources and noise models that are considered here. However, with different choices of average input energy and resource squeezing, the average fidelity may get affected differently. Nevertheless, as in the noiseless scenario, we can get a quantum advantage over the classical one when the input energy or resource squeezing is reasonably high.

Impact of measurement noise on average fidelity. We observe that the average fidelity decreases monotonically with \mathcal{R} , for all types of resources and as well as inputs. This is quite expected since in general noise causes some hindrance in any protocol. However, three interesting features emerge which are discussed as follows (see Fig. 6).

- Considering only \mathcal{F} , Gaussian shared channels are again more robust against measurement noise in absence of resource noise, i.e., $\tau = 0$ as compared to non-Gaussian ones. More precisely, for coherent states as inputs, the difference between \mathcal{F} at low and high values of measurement noise is prominent for low input average energy and high resource squeezing while for squeezed-coherent state, this feature is noticeable at high average energy of the input. E.g. when $\sigma_c = 1.0$ and $r = 1.5$, we define $\delta\mathcal{F} = \mathcal{F}^{\mathcal{R}=0.0} - \mathcal{F}^{\mathcal{R}=4.0}$ which for TMSV is $\delta\mathcal{F}_{TMSV} = 0.133$, for PA is $\delta\mathcal{F}_{PA} = 0.165$ and for PS, $\delta\mathcal{F}_{PS} = 0.163$.

Typically, we expect that to obtain a better average fidelity with a fixed average energy, we require a resource with high squeezing. However, we observe an opposite behavior with coherent states as inputs and PS states as quantum channel in presence of a noise only in measurements (i.e., taking $\tau = 0.0$). For example, with $\sigma_c = 1.0$, beyond $\mathcal{R} \sim 0.35$, the low resource squeezing helps to manage better average fidelity than the states with high squeezing. A similar trend is also observed in case of teleporting squeezed input states with TMSV and PS resource although the quantum advantage is unattainable there.

- Another point of interest is the ‘constructive effect’ of noise that we have already noted in case of uniform distribution of the input states. Moreover, as in the constrained uniform distribution, it is noted that the constructive effect starts at relatively lower values of \mathcal{R} for non-Gaussian resources compared to the Gaussian ones irrespective of squeezed or coherent states as inputs. E.g. considering $r = 1.5$ and $\sigma_c = 1.0$, constructive effect emerges with the measurement noise values for different shared states as $\mathcal{R}_{TMSV} \sim 0.40$, $\mathcal{R}_{PA} \sim 0.26$, $\mathcal{R}_{PS} \sim 0.28$.
- Resources with lower squeezing strength corresponding to a fixed input distribution are less sensitive against measurement noise. This feature can easily be noted from Fig. 6 when we compare $r = 1.0$ and 1.5 for a fixed standard deviation. Moreover, noisy channels help to retain the robustness against the noise in measurement.

Response against resource noise. As seen in case of constrained uniform distribution, \mathcal{F} exhibits some distinct features in this noise model which are either not observed or not pronounced in presence of noise in measurements.

- Greater average energy of the input states makes the performance of the protocol less robust against resource noise. The measurement noise slightly improves the robustness of the performance against the resource noise.
- We can see that with small values of σ_c (~ 1.0) for coherent states as input, non-Gaussian resources are more robust than the Gaussian one against resource noise (see Fig. 6) while Gaussian states are the best for input

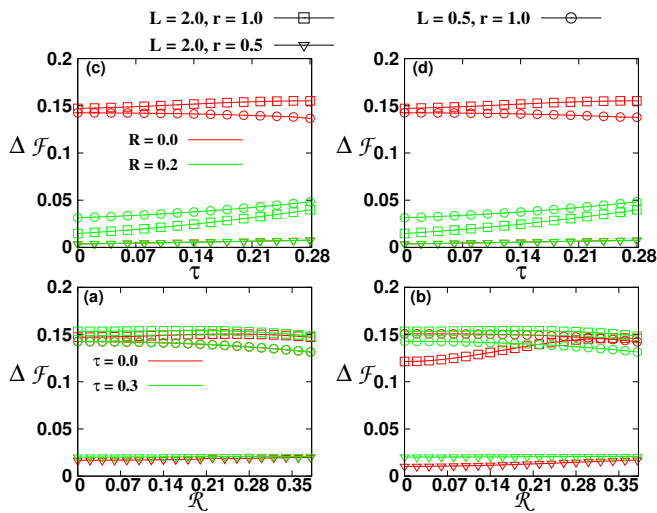


FIG. 7. Fidelity deviation, $\Delta\mathcal{F}$ (vertical axis) against noise parameters, \mathcal{R} (lower panel), and τ (upper panel) (horizontal axis) for squeezed-coherent input states. The energy cut-off and resource squeezing are depicted as $L = 2.0 = 1.0, r = 1.0$ (hollow squares), $L = 2.0, r = 0.5$ (hollow triangles) and $L = 0.5, r = 1.0$ (hollow circles). All other specifications are the same as in Fig. 6. All the axes are dimensionless.

squeezed and squeezed-coherent states in the high input energy regime.

Summarizing, we find that in a noisy scenario, both TMSV and PS states are good quantum channels for QT according to the average fidelity regardless of energy distribution of inputs and input states. It will now be interesting to enquire whether the patterns of fidelity deviation can help us to identify the suitable resource for QT.

VI. ROLE OF FIDELITY DEVIATION FOR NOISY TELEPORTATION

We now shift our attention to the behavior of fidelity deviation against two noise parameters, \mathcal{R} , and τ . In particular, we illustrate the behaviour of $\Delta\mathcal{F}$ with respect to resource noise (measurement noise) at a fixed measurement noise (resource noise) for coherent, squeezed and squeezed coherent states respectively as input.

Constrained uniform input distribution. Let us enumerate some of the interesting observations below as depicted in Fig. 7.

1. *Constancy of fidelity deviation.* The first interesting observation is that $\Delta\mathcal{F}$ remains almost constant with the increase of noise, especially when the variation of \mathcal{R} for a fixed value of τ is studied. A slight increase is seen with the change of τ .
2. *Dependence of input energy on deviation.* $\Delta\mathcal{F}$ possesses a high value for all resource states, across moderate values of \mathcal{R} and τ when the input energy is high and the squeezing is moderate.

3. *Measurement noise vs. resource noise.* Focusing on the variation of $\Delta\mathcal{F}$ against the measurement inefficiency, we find that at moderate values of the resource noise, e.g. $\tau = 0.3$, the deviation is higher than that of the case with $\tau = 0$ across the entire range of \mathcal{R} except some situations with squeezed coherent input states. Thus there is no counteracting effect of one noise on the other, as in the case of average fidelity. In contrast, if we consider $\Delta\mathcal{F}$ with a nonvanishing moderate value of \mathcal{R} , say 0.2, it is less for all values of τ for Gaussian as well as non-Gaussian states compared to the situation with vanishing \mathcal{R} (as depicted in Fig. 7), thereby exhibiting constructive effects also in fidelity deviation.

4. *Optimal channels.* Scrutinizing the behavior of fidelity deviation, we observe that even in presence of the noise models considered here, non-Gaussian states give low fidelity deviation compared to that obtained from the Gaussian ones. Among non-Gaussian states, photon added states give low fidelity deviation than that of the photon subtracted ones like the noiseless situation. However, it is important to note that PA states rarely give any quantum advantage according to the average fidelity and hence such a low fidelity deviation does not lead to any benefit in QT.

Role of Gaussian input distribution. Let us compare the trends of $\Delta\mathcal{F}$ obtained for inputs chosen from the Gaussian distribution with the uniform distribution discussed above by varying \mathcal{R} and τ .

First of all, the variation of $\Delta\mathcal{F}$ observed with \mathcal{R} and τ having low input energy is more than that obtained in constrained uniform case for different inputs.

Secondly, except TMSV states in which high energy sometimes gives low $\Delta\mathcal{F}$, the relation between input energy and the deviation observed in the uniform distribution remains same for the Gaussian distribution.

Thirdly, like the uniform distribution, with the increase of τ from a vanishing value to a moderate one, deviation always increases for coherent input states while for squeezed coherent state, there are some exceptional regions where the opposite picture emerges for all three quantum channels. However, unlike uniform distribution, the increase of \mathcal{R} does not lead to low fidelity deviation in this case with the variation of τ – it remains almost constant with τ after the increase of \mathcal{R} which can be justified by inspecting Fig. 8.

Finally, analysing both the fidelity and its deviation along with input energy distributions, one cannot identify a single channel which are more suitable for QT than the others. Specifically, our study reveals that in presence of noise in measurements as well as channels, there is a competition between non-Gaussian photon subtracted and the Gaussian TMSV states which give the quantum advantage in QT depending on the energy of the input ensembles.

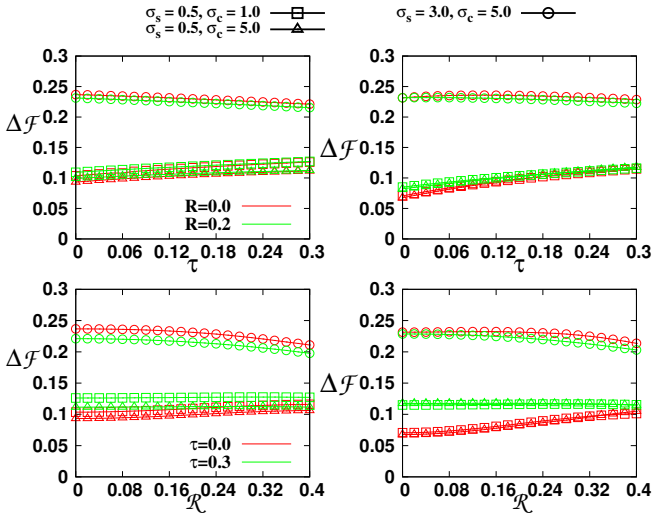


FIG. 8. $\Delta\mathcal{F}$ (ordinate) by varying \mathcal{R} (lower panel) and τ (upper panel) (abscissa) for squeezed-coherent states as inputs drawn from a Gaussian distribution using TMSV (left panel) and PS (right panel) as shared channels. We depict the standard deviation parameters as $\sigma_s = 0.5, \sigma_c = 1.0$ (hollow squares), $\sigma_s = 0.5, \sigma_c = 5.0$ (hollow triangles), $\sigma_s = 3.0, \sigma_c = 5.0$ (hollow circles). Here we consider the resource squeezing $r = 1.0$. All other specifications are the same as in Fig. 6. All axes are dimensionless.

VII. CONCLUSION

Quantum teleportation is one of the most researched information theoretic protocols, both in terms of its theoretical foundations, as well as experimental implementations. Traditionally, the performance of quantum teleportation is assessed using the average fidelity. Recently in discrete variable quantum teleportation, it was shown that the standard deviation of fidelity, namely the fidelity deviation, can non-trivially alter the calibration of the performance in teleportation.

In this work, we have introduced the concept of fidelity deviation in continuous variable (CV) quantum teleportation (QT) both for the ideal and noisy cases. In CV teleportation, the concept of average fidelity and fidelity deviation, when considered as a direct continuation from the case of discrete variables, suffer from energetic divergences. We presented regularized versions of these quantities, free from such divergences, by considering that the set of states to be teleported are constrained to have a finite energy cut-off or by introducing Gaussian suppression of the input energy. In particular, for the constrained uniform distribution with a fixed energy threshold, states are drawn with equal probability over all energy values under the threshold, and for the Gaussian ensemble a fixed standard deviation determines the average energy range of the input set.

In ideal CV teleportation, we first reported the general trends of average fidelity and fidelity deviation for both the considered constrained uniform and Gaussian distributions of inputs for both Gaussian and non-Gaussian shared states between the sender and the receiver. In the noiseless scenario, we observed that the average fidelity decreases with the en-

ergy of the input state at a fixed value of the resource squeezing. The fidelity deviation too suffers from the rise in ensemble energy, such that it is more for input states of higher energy compared to the inputs having low energy cut-offs. However, the effect of ensemble energy is different on different resource states. We found that the photon added (PA) state is the least useful resource since it can overcome the classical bound only at large values of the input energy. The situation improves for increased resource squeezing, but the photon subtracted (PS) state as well as the Gaussian TMSV state perform far better than the PA state. The PS state is the most efficient resource since it provides the highest average fidelity for highly energetic input sets with reasonably low fidelity deviation, although the PA state furnishes the minimum value in this regard. Overall, advantage is offered by non-Gaussian states for both the figures of merit and the PS state establishes itself as the go-to resource. We also showed how fidelity deviation can non-trivially alter the hierarchy among resource states for which the average fidelities behave almost identically.

Noise is inevitable in any experiment, and many developments have been made to study the effect of noise on the primary figure of merit - the average fidelity. We further the investigation into the noisy teleportation process by including the second moment of the fidelity statistics. Our work focuses on the behavior of the aforementioned figures of merit with respect to the input ensembles which are characterised by their energy distribution. We also considered the impact of noise present in the channels as well as measurements on fidelity statistics. Interestingly, we found that both kinds of noise are seen to affect the non-Gaussian states to a greater extent, in a sense that their average fidelity falls at a much faster rate, thereby making the TMSV state the best resource, especially at higher input energies. The difference in the sources of noise leads to a constructive effect - the resource noise is able to counter the effects of imperfection in measurements, due to which the average fidelity for a higher value of the resource noise is better than that at a lower value of the same, when studied against the variation of the noise. The resource noise also affects the teleportation protocol to a lesser extent, since the figures of merit change very slowly with respect to its variations. Moreover, the effects of noise are less pronounced in case of low energy input ensembles and high squeezing strength of the available resources. In case of the input states, we report that the coherent state suffers much less due to noise, as compared to the squeezed and squeezed-coherent ensembles.

Our work analyses the performance of CV teleportation protocol in the new light of the regularized version of both average fidelity and fidelity deviation. We demonstrate how incorporating this additional quantifier (fidelity deviation) can provide fundamental insights into the classification of shared channels for QT that the average fidelity alone cannot capture both in noiseless and noisy scenarios. We believe that the present work opens new avenues into research on CV teleportation.

ACKNOWLEDGMENTS

We acknowledge the support from the Interdisciplinary Cyber Physical Systems (ICPS) program of the Depart-

ment of Science and Technology (DST), India, Grant No.: DST/ICPS/QuST/Theme- 1/2019/23, the use of `QIClib` – a modern C++ library for general purpose quantum information processing and quantum computing (<https://titaschanda.github.io/QIClib>).

-
- [1] C. H. Bennett, G. Brassard, C. Crépeau, R. Jozsa, A. Peres, and W. K. Wootters, *Phys. Rev. Lett.* **70**, 1895 (1993).
- [2] M. Horodecki, P. Horodecki, and R. Horodecki, *Phys. Rev. A* **60**, 1888 (1999).
- [3] R. Horodecki, M. Horodecki, and P. Horodecki, *Physics Letters A* **222**, 21 (1996).
- [4] F. Verstraete and H. Verschelde, *Phys. Rev. Lett.* **90**, 097901 (2003).
- [5] S. L. Braunstein and A. Mann, *Phys. Rev. A* **51**, R1727 (1995).
- [6] R. Gupta, S. Gupta, S. Mal, and A. Sen(De), *Phys. Rev. A* **103**, 032608 (2021).
- [7] P. Horodecki, M. Horodecki, and R. Horodecki, *Phys. Rev. Lett.* **82**, 1056 (1999).
- [8] D. Bouwmeester, J.-W. Pan, K. Mattle, M. Eibl, H. Weinfurter, and A. Zeilinger, *Nature* **390**, 575 (1997).
- [9] R. Ursin, T. Jennewein, M. Aspelmeyer, R. Kaltenbaek, M. Lindenthal, P. Walther, and A. Zeilinger, *Nature* **430**, 849 (2004).
- [10] H. Krauter, D. Salart, C. A. Muschik, J. M. Petersen, H. Shen, T. Fernholz, and E. S. Polzik, *Nature Physics* **9**, 400 (2013).
- [11] D. Boschi, S. Branca, F. De Martini, L. Hardy, and S. Popescu, *Phys. Rev. Lett.* **80**, 1121 (1998).
- [12] R. Valivarthi, M. G. Puigibert, Q. Zhou, G. H. Aguilar, V. B. Verma, F. Marsili, M. D. Shaw, S. W. Nam, D. Oblak, and W. Tittel, *Nature Photonics* **10**, 676 (2016).
- [13] X.-L. Wang, X.-D. Cai, Z.-E. Su, M.-C. Chen, D. Wu, L. Li, N.-L. Liu, C.-Y. Lu, and J.-W. Pan, *Nature* **518**, 516 (2015).
- [14] N. Lee, H. Benichi, Y. Takeda, S. Takeda, J. Webb, E. Huntington, and A. Furusawa, *Science* **332**, 330 (2011).
- [15] Q. Zhang, A. Goebel, C. Wagenknecht, Y.-A. Chen, B. Zhao, T. Yang, A. Mair, J. Schmiedmayer, and J.-W. Pan, *Nature Physics* **2**, 678 (2006).
- [16] X.-M. Jin, J.-G. Ren, B. Yang, Z.-H. Yi, F. Zhou, X.-F. Xu, S.-K. Wang, D. Yang, Y.-F. Hu, S. Jiang, T. Yang, H. Yin, K. Chen, C.-Z. Peng, and J.-W. Pan, *Nature Photonics* **4**, 376 (2010).
- [17] A. Furusawa, J. L. Sørensen, S. L. Braunstein, C. A. Fuchs, H. J. Kimble, and E. S. Polzik, *Science* **282**, 706 (1998).
- [18] X.-X. Xia, Q.-C. Sun, Q. Zhang, , and J.-W. Pan, *Quantum Science and Technology* **3**, 014012 (2017).
- [19] H. Takesue, S. D. Dyer, M. J. Stevens, V. Verma, R. P. Mirin, and S. W. Nam, *Optica* **2**, 832 (2015).
- [20] M. Studziński, S. Strelchuk, M. Mozrzyk, and M. Horodecki, *Scientific Reports* **7**, 10871 (2017).
- [21] X. Jeong, J. Kim, and S. Lee, *Phys. Rev. A* **102**, 012414 (2020).
- [22] M. Christandl, F. Leditzky, C. Majenz, G. Smith, F. Speelman, and M. Walter, *Communications in Mathematical Physics* **381**, 379 (2021).
- [23] M. T. Quintino, *Quantum Views* **5**, 56 (2021).
- [24] J. Zhang, C. Xie, and K. Peng, *Journal of Optics B: Quantum and Semiclassical Optics* **3**, 293 (2001).
- [25] J. Koga, G. Kimura, and K. Maeda, *Phys. Rev. A* **97**, 062338 (2018).
- [26] G. L. Zanin, M. J. Jacquet, M. Spagnolo, P. Schiansky, I. A. Calafell, L. A. Rozema, and P. Walther, *Opt. Express* **29**, 3425 (2021).
- [27] M. Caleffi and A. S. Cacciapuoti, *IEEE Journal on Selected Areas in Communications* **38**, 575 (2020).
- [28] M. Mura, D. Jonathan, M. B. Plenio, and V. Vedral, *Phys. Rev. A* **59**, 156 (1999).
- [29] A. Sen(De) and U. Sen, *Phys. Rev. A* **81**, 012308 (2010).
- [30] Q. Wang, W. Li, Y. Wu, W. Yao, F. Li, L. Tian, Y. Wang, and Y. Zheng, *Phys. Rev. A* **104**, 032419 (2021).
- [31] S. Roy, T. Das, D. Das, A. Sen(De), and U. Sen, *Annals of Physics* **422**, 168281 (2020).
- [32] S. Roy, A. Bera, S. Mal, A. Sen (De), and U. Sen, (2019), 1905.04164.
- [33] J. Bang, J. Ryu, and D. Kaszlikowski, *Journal of Physics A: Mathematical and Theoretical* **51**, 135302 (2018).
- [34] H. Jeong and M. S. Kim, *Phys. Rev. A* **65**, 042305 (2002).
- [35] T. C. Ralph, A. Gilchrist, G. J. Milburn, W. J. Munro, and S. Glancy, *Phys. Rev. A* **68**, 042319 (2003).
- [36] A. Ghosal, D. Das, S. Roy, and S. Bandyopadhyay, *Journal of Physics A: Mathematical and Theoretical* **53**, 145304 (2020).
- [37] A. Ghosal, D. Das, S. Roy, and S. Bandyopadhyay, *Phys. Rev. A* **101**, 012304 (2020).
- [38] S. Roy and A. Ghosal, *Phys. Rev. A* **102**, 012428 (2020).
- [39] S. Roy, S. Mal, and A. Sen(De), *Phys. Rev. A* **105**, 022610 (2022).
- [40] S. Pirandola, J. Eisert, C. Weedbrook, A. Furusawa, and S. L. Braunstein, *Nature Photonics* **9**, 641 (2015).
- [41] U. L. Andersen, T. Gehring, C. Marquardt, and G. Leuchs, *Physica Scripta* **91**, 053001 (2016).
- [42] J. Nokkala, R. Martínez-Peña, G. L. Giorgi, V. Parigi, M. C. Soriano, and R. Zambrini, *Communications Physics* **4**, 53 (2021).
- [43] A. Ferraro, S. Olivares, and M. G. A. Paris, (2005), [quant-ph/0503237](https://arxiv.org/abs/quant-ph/0503237).
- [44] G. Adesso, S. Ragy, and A. R. Lee, *Open Systems & Information Dynamics* **21**, 1440001 (2014).
- [45] A. Serafini, *Quantum Continuous Variables*, 1st ed. (CRC Press, 2017).
- [46] L. Vaidman, *Phys. Rev. A* **49**, 1473 (1994).
- [47] S. L. Braunstein and H. J. Kimble, *Phys. Rev. Lett.* **80**, 869 (1998).
- [48] F. Dell’Anno, S. De Siena, L. Albano Farias, and F. Illuminati, *The European Physical Journal Special Topics* **160**, 115 (2008).
- [49] F. Dell’Anno, S. De Siena, L. Albano, and F. Illuminati, *Phys. Rev. A* **76**, 022301 (2007).
- [50] E. Villasenor and R. Malaney, [arXiv:2111.00672](https://arxiv.org/abs/2111.00672) (2021).
- [51] E. Villasenor, M. He, Z. Wang, R. Malaney, and M. Z. Win, *IEEE Transactions on Quantum Engineering* **2**, 1 (2021).
- [52] S. Wang, L.-L. Hou, X.-F. Chen, and X.-F. Xu, *Phys. Rev. A* **91**, 063832 (2015).
- [53] A. Kitagawa, M. Takeoka, M. Sasaki, and A. Chefles, *Phys. Rev. A* **73**, 042310 (2006).
- [54] S. Olivares, M. G. A. Paris, and R. Bonifacio, *Phys. Rev. A* **67**, 032314 (2003).
- [55] P. T. Cochrane, T. C. Ralph, and G. J. Milburn, *Phys. Rev. A* **65**, 062306 (2002).

- [56] T. Opatrny, G. Kurizki, and D.-G. Welsch, *Phys. Rev. A* **61**, 032302 (2000).
- [57] F. Dell’Anno, S. De Siena, and F. Illuminati, *Phys. Rev. A* **81**, 012333 (2010).
- [58] T. J. Johnson, S. D. Bartlett, and B. C. Sanders, *Phys. Rev. A* **66**, 042326 (2002).
- [59] H. Yonezawa, T. Aoki, and A. Furusawa, *Nature* **431**, 430 (2004).
- [60] A. Furusawa, in *Int. Quant. Electronics Conf.* (2005) pp. 1122–1123.
- [61] P. van Loock and S. L. Braunstein, *Phys. Rev. Lett.* **84**, 3482 (2000).
- [62] H. S. Dhar, A. Chatterjee, and R. Ghosh, *Journal of Physics B: Atomic, Molecular and Optical Physics* **48**, 185502 (2015).
- [63] H.-J. Kim, J. Kim, and H. Nha, *Phys. Rev. A* **88**, 032109 (2013).
- [64] H. Nha, S.-Y. Lee, S.-W. Ji, and M. S. Kim, *Phys. Rev. Lett.* **108**, 030503 (2012).
- [65] E. P. Menzel, R. Di Candia, F. Deppe, P. Eder, L. Zhong, M. Ihmig, M. Haerberlein, A. Baust, E. Hoffmann, D. Ballester, K. Inomata, T. Yamamoto, Y. Nakamura, E. Solano, A. Marx, and R. Gross, *Phys. Rev. Lett.* **109**, 250502 (2012).
- [66] A. G. and F. Illuminati, (2007), [quant-ph/0510052](#).
- [67] N. Takei, N. Lee, D. Moriyama, J. S. Neergaard-Nielsen, and A. Furusawa, *Phys. Rev. A* **74**, 060101 (2006).
- [68] A. Dolińska, B. C. Buchler, W. P. Bowen, T. C. Ralph, and P. K. Lam, *Phys. Rev. A* **68**, 052308 (2003).
- [69] G. Adesso and F. Illuminati, *Phys. Rev. Lett.* **99**, 150501 (2007).
- [70] S. Pirandola and S. Mancini, *Laser Physics* **16**, 1418 (2006).
- [71] G. Chiribella and G. Adesso, *Phys. Rev. Lett.* **112**, 010501 (2014).
- [72] H. Vahlbruch, M. Mehmet, K. Danzmann, and R. Schnabel, *Physical Review Letters* **117** (2016), [10.1103/physrevlett.117.110801](#).
- [73] N. Linden and S. Popescu, *Phys. Rev. A* **59**, 137 (1999).
- [74] P. van Loock, *Fortschr. Phys.* **50**, 1117 (2002).
- [75] S. L. Braunstein, C. A. Fuchs, and H. J. Kimble, *Journal of Modern Optics* **47**, 267 (2000).
- [76] J.-X. Zhang, C.-D. Xie, and K.-C. Peng, *Chinese Physics Letters* **22**, 3005 (2005).
- [77] A. Serafini, O. C. O. Dahlsten, and M. B. Plenio, *Phys. Rev. Lett.* **98**, 170501 (2007).
- [78] G. Adesso and G. Chiribella, *Phys. Rev. Lett.* **100**, 170503 (2008).
- [79] F. Dell’Anno, S. De Siena, G. Adesso, and F. Illuminati, *Phys. Rev. A* **82**, 062329 (2010).